



Research article

Molecular characterisation of ILRUN, a novel inhibitor of proinflammatory and antimicrobial cytokines



Rebecca L. Ambrose^{a,1,3}, Aaron M. Brice^{a,3}, Alessandro T. Caputo^b, Marina R. Alexander^a, Leon Tribolet^a, Yu Chih Liu^{b,2}, Timothy E. Adams^b, Andrew G.D. Bean^a, Cameron R. Stewart^{a,*}

^a CSIRO Health & Biosecurity, Australian Centre for Disease Preparedness, Geelong, Victoria, 3220, Australia

^b CSIRO Manufacturing, Parkville, Victoria, 3010, Australia

ARTICLE INFO

Keywords:

Immunology
Inflammation
Infectious disease
Immune response
Viruses
Biochemistry
Biomolecules
ILRUN
C6orf106
Innate immunity
Interferon
p300
CBP

ABSTRACT

Regulation of type-I interferon (IFN) production is essential to the balance between antimicrobial defence and autoimmune disorders. The human protein-coding gene ILRUN (inflammation and lipid regulator with UBA-like and NBR1-like domains, previously C6orf106) was recently characterised as an inhibitor of antiviral and proinflammatory cytokine (interferon-alpha/beta and tumor necrosis factor alpha) transcription. Currently there is a paucity of information about the molecular characteristics of ILRUN, despite it being associated with several diseases including virus infection, coronary artery disease, obesity and cancer. Here, we characterise ILRUN as a highly phylogenetically conserved protein containing UBA-like and a NBR1-like domains that are both essential for inhibition of type-I interferon and tumor necrosis factor alpha) transcription in human cells. We also solved the crystal structure of the NBR1-like domain, providing insights into its potential role in ILRUN function. This study provides critical information for future investigations into the role of ILRUN in health and disease.

1. Introduction

The type-I interferon (IFN) response provides a robust innate immune defence against pathogens, instigated by the detection of pathogen-associated molecular patterns (PAMPs) such as foreign nucleic acid and bacterial lipopolysaccharide (LPS) (McNab et al., 2015). PAMPs are detected by intracellular sensor proteins called pathogen recognition receptors (PRRs), including toll-like receptors (TLRs) and retinoic acid-inducible gene I (RIG-I)-like receptors (RLRs), amongst others (McNab et al., 2015). PRR-induced signalling pathways result in the activation of the latent transcription factors IFN regulatory factor 3 (IRF3), IRF7 (following prolonged stimulation), and nuclear factor kappa-light-chain-enhancer of activated B-cells (NFκB), which initiate the transcription of type-I IFNs (IFN α and IFN β) and the proinflammatory cytokines interleukin (IL)-6 and tumor necrosis factor- α (TNF α) (McNab

et al., 2015). These secreted factors act in an autocrine and paracrine manner to induce expression of antimicrobial proteins as well as activate and recruit immune cells, promoting pathogen clearance (McNab et al., 2015). Due to the profound effects of these signalling proteins on cell biology, the type-I IFN response is tightly regulated by numerous mechanisms to prevent aberrant signalling that can promote many disease states, including inflammation, autoimmunity and cancer (Chen et al., 2017; Fuertes et al., 2013; Motwani et al., 2019; Rodero and Crow, 2016; Snell et al., 2017).

We recently characterised a novel inhibitor of the type-I IFN response, C6orf106, which promotes the degradation of the transcriptional coactivators p300 and cAMP-response element-binding protein-binding protein (CBP) within the nucleus and inhibits IRF3-DNA binding, resulting in significantly impaired transcription of type-I IFNs and TNF α , but not IL-6 (Ambrose et al., 2018). Based on our

* Corresponding author.

E-mail address: Cameron.Stewart@csiro.au (C.R. Stewart).

¹ Present address: Centre for Innate Immunity and Infectious Diseases, Hudson Institute of Medical Research, Clayton, Victoria, 3168, Australia.

² Present address: CSL Behring, Broadmeadows, Victoria, 3047, Australia.

³ These authors contributed equally.

data, and those of others (Bi et al., 2020), this protein was renamed Inflammation and Lipid Regulator with UBA-like and NBR1-like domains (ILRUN). Genome-wide analyses have also identified the *ILRUN* gene as a body mass index (BMI)-associated locus and positive correlations between *ILRUN* expression and the malignancy and invasiveness of several cancers have been identified (Baranski et al., 2018; Jiang et al., 2015; Li et al., 2019; Riveros-McKay et al., 2019; Zhang et al., 2015). The latter studies postulate that ILRUN promotes the extracellular signal-related kinases (ERK) signalling pathway, reducing expression of the cell adhesins E-cadherin and p120ctn, thereby promoting metastasis (Li et al., 2019; Zhang et al., 2015). This suggests that ILRUN may be of importance to several diseases of significant concern to human health and, therefore, an attractive therapeutic target. At present, however, there is limited information on the molecular and structural biology of ILRUN.

In this report, we characterise ILRUN using bioinformatic, expression analysis and experimental approaches. We show that the N-terminal ubiquitin-associated (UBA)-like and central neighbour of BRCA1 gene 1 (NBR1)-like domains are evolutionarily well-conserved in animals, and both these domains contribute to ILRUN-mediated inhibition IRF3 signalling; the C-terminal disordered region, whose sequence is much more disparate, appears dispensable for this function. We also present a crystal structure of the NBR1-like domain and a structure prediction of the UBA-like domain, in addition to performing expression analysis from published datasets to elucidate ILRUN expression in different human tissues and immune cell types, identifying ILRUN as appearing to be most abundant in testis and activated B-cells. Together, these data advance our knowledge of ILRUN biology and its roles in human health and disease.

2. Materials and methods

2.1. Cells

HeLa cells (ATCC CCL-2) were maintained in Eagle's minimum essential medium (EMEM) supplemented with 10% (v/v) fetal bovine serum (FBS), 10 mM HEPES, 2 mM L-glutamine, 100 units/mL penicillin, and 100 µg/mL streptomycin (Thermo Fisher Scientific). All cells were kept at 37 °C in a humidified incubator (5% CO₂).

2.2. *ILRUN* mutant plasmid generation

The ΔUBA and Δdisordered (Δdis) coding sequences were amplified from the pre-existing pCAGGS-ILRUN-FLAG vector (expressing C-terminally FLAG-tagged human ILRUN), previously described in (Ambrose et al., 2018), using forward and reverse primers as in Supplementary Table A1. The ΔNBR1 coding sequence was designed upon the naturally occurring isoform ILRUNb (NCBI NP_073595.2) and was synthesised by GenScript with a C-terminal FLAG coding sequence. All amplicons were ligated into the mammalian expression vector pCAGGS using the *SacI* and *XhoI* restriction sites and transformed into chemically competent *Escherichia coli* (MAX Efficiency DH5α competent cells, Thermo Fisher Scientific, Massachusetts, United States). Following Sanger sequencing to confirm correct sequences, plasmids were propagated in DH5α *E.coli* and purified using a Qiagen (Hilden, Germany) EndoFree Plasmid Maxi kit as specified by the manufacturers.

2.3. DNA transfection and poly(I:C) stimulation

HeLa cells in 24-well plates were reverse transfected with 300 ng of endotoxin free plasmid DNA and 1 µL Lipofectamine 2000 in OptiMEM (Thermo Fisher Scientific) as previously described. Cells were stimulated with 5 µg/mL high molecular weight poly(I:C) (Invivogen, California, United States) by transfection (1.5 µL Lipofectamine 2000) for 6 h.

2.4. RNA purification, reverse transcription, and quantitative real-time PCR

HeLa cells were lysed in TRIzol (Thermo Fisher Scientific), and RNA was extracted according to the manufacturer's protocols. Following DNase treatment (RNase-free DNase, Promega, Wisconsin, United States), 500 ng of RNA was reverse-transcribed to DNA using SensiFast reverse transcriptase (Bioline, London, United Kingdom) first-strand cDNA synthesis protocols. Quantitative reverse-transcription polymerase chain reaction (qRT-PCR) was performed using SYBR Green (Applied Biosystems, California, United States) on a StepOne Plus PCR cycler (Applied Biosystems). PCR cycling for gene detection was at 95 °C for 10 min followed by 45 cycles of 95 °C for 15 sec and 60 °C for 1 min. A melting curve analysis was performed to eliminate primer-dimer artefacts and to verify the specificity of the assay. Cytokine expression was assayed using the ΔΔCT method and normalized to GAPDH. Primers used in qRT-PCR analyses are as previously described (Ambrose et al., 2018).

2.5. IRF3 DNA binding assays and IFN-β ELISA

HeLa cells were reverse-transfected in 6 cm dishes (as described above but scaled up according to dish size) for 18 h then stimulated with transfected poly(I:C) for 6 h. Cells were incubated on ice in hypotonic buffer (20 mM HEPES, 5 mM NaF, 10 µM Na₂MoO₄, 0.1 mM EDTA) for 15 min followed by cytoplasmic membrane disruption with 0.1% Nonidet P-40. Nuclei were pelleted at 12,000 × g for 30 sec, washed in hypotonic buffer, and lysed in complete lysis buffer on ice for 45 min (supplemented with phosphatase and protease inhibitors and DTT, Abcam, Cambridge, United Kingdom). Debris was removed by centrifugation and nuclear protein extracts were quantified using a bicinchoninic acid assay (Pierce, Massachusetts, United States). 10 µg of nuclear protein (in duplicate) was applied to an IRF3 transcription factor assay plate (ab207210, Abcam) and DNA binding was assayed as indicated by the manufacturer. Supernatants collected from transfected cells were assayed for IFN-β secretion using a sandwich ELISA kit (elisakit.com, Victoria, Australia) according to the manufacturer's protocols. IFN-β concentrations were calculated by comparison with standards using a polynomial regression method.

2.6. Crystallisation of ILRUN NBR1 domain

The full-length ILRUN gene was synthesised with codon-optimisation for *E. coli* expression and sub-cloned into pET43 with a C-terminal His₆-tag. The construct was transformed into BL21 (DE3) cells and grown in Terrific Broth with 100 µg/mL carbenicillin (GoldBio, Missouri, United States) at 37 °C to an OD₆₀₀ = 1.1. Expression was induced with 1 mM isopropyl-β-D-thiogalactopyranoside (GoldBio) and left for 3 h before harvesting at 5000 × g for 10 min. For a wet pellet weight of 25 g, 100 mL of lysis buffer (20 mM Tris-HCl, pH 8.0, 300 mM NaCl, 2 mM MgCl₂, 10 mM imidazole). The lysis buffer was supplemented with ~20 U/mL of Benzonase Nuclease (MerckMillipore) and 2 cOmplete EDTA-free protease inhibitor tablets (Roche, Basel, Switzerland) before lysing with three passes through an EmulsiFlex C-5 (Avestin, Ontario, Canada) at 15,000 psi. The lysate was cleared by centrifugation at 48,000 g. The supernatant was loaded onto an ÄKTAexpress (along with all columns, GE Lifesciences, Illinois, United States) with the following three step program: 1) 1 mL HisTrap crude washed with 20 column volumes of wash buffer (20 mM Tris-HCl, pH 8.0, 300 mM NaCl, 20 mM imidazole) and eluted with 5 column volumes of elution buffer (20 mM Tris-HCl, pH 8.0, 300 mM NaCl, 250 mM imidazole). The following two steps use buffer A (20 mM Tris-HCl, pH 8.0) and B (20 mM Tris-HCl, pH 8.0, 1000 mM NaCl). 2) The eluate was automatically loaded onto a HiPrep 16/10 Desalt run in 5% B. 3) and the protein peak was collected to inject into a 1 mL HiTrap Q HP column. After a 20 column volume wash at 5% B, the protein was eluted in a 5–50% B gradient over 20 column volumes. The ILRUN-containing peak was finally polished and assessed for homogeneity on a Superdex 75 16/600 column in 20 mM Tris-HCl, 8.0, 150 mM NaCl. Typically, the final yield was between 0.5 and 1.0 mg/L of culture.

Small crystals were readily obtained from many conditions in sparse matrix vapour diffusion experiments with *in situ* chymotrypsin treatment. To obtain larger, single crystals, a small quantity of the full-length ILRUN was treated with chymotrypsin (Sigma Aldrich, Missouri, United States) in a 30:1 (w:w) ILRUN:chymotrypsin ratio for 1 h at room temperature. The proteolysis was stopped with addition of 1 mM PMSF and the NBR1 domain isolated by gel filtration as above. The appropriate fractions were concentrated in an Amicon Ultra-4 3 kDa MWCO ultrafiltration device (MerckMillipore, Massachusetts, United States) to $A_{280} = 3.0$. Single crystals were obtained by mixing 150 nL with 30 nL of seeds made from small crystals mentioned above and 120 nL of 1 M ammonium sulfate and 0.15 M trisodium citrate-citric acid, pH 5.5. Drops containing thin single plates had an equal volume of 3 M sodium malonate, pH 5.5, added, before being harvested and flash cooled in liquid nitrogen.

Diffraction experiments were measured at the MX2 beamline at the Australian Synchrotron (Clayton, Australia) at a wavelength of 1.45865 Å. Images were processed using autoPROC (Tickle et al., 2018; Vonrhein et al., 2011) which indexed and integrated with XDS (Kabsch, 2010) and then scaled and merged with Pointless, Aimless and Truncate from the CCP4 suite (Winn et al., 2011). Automated molecular replacement was carried out with MrBUMP with the most favourable solution that was used for model building being chain A of the PDB entry 4OLE. The model was iteratively built with cycles of Coot and autoBUSTER using local secondary structure restraints (Bricogne et al., 2017; Smart et al., 2012). The model was validated with Molprobity (Williams et al., 2018).

2.7. Transcript expression data mining

The mined transcript expression data analysed and compiled by the May'ayan Lab, Mount Sinai Center for Bioinformatics was downloaded from their ARChS4 website (amp.pharm.mssm.edu/archs4/download.html) (Lachmann et al., 2018). Published RNA-seq datasets were selected based on the following criteria: i) contained >3 healthy control replicates, ii) were >1000 MBases in size and iii) were derived from a tissue or immune cell type of interest. Metadata associated with each sequence read archive was downloaded from the Gene Expression Omnibus (www.ncbi.nlm.nih.gov/geo/) and R scripts were written to extract associated *ILRUN* isoform expression levels.

2.8. Statistics

The difference between multiple groups was analysed by one- or two-way ANOVA with Bonferroni post-test. A *P* value of <0.05 was considered significant.

3. Results

3.1. Description of ILRUN genomic organisation of ILRUN locus

The human *ILRUN* gene (Figure 1A) is located on chromosome 6 (locus p21.31) and flanked by genes encoding SAM pointed domain-containing ETS transcription factor (SPDEF) and small nuclear ribonucleoprotein polypeptide C (SNRPC). SPDEF is a transcription factor expressed in prostate, trachea and colon epithelium that is involved in differentiation and overexpressed in prostate and breast cancers, while SNRPC is a component of the U1 small nuclear ribonucleoprotein spliceosome that functions pre-mRNA processing (Singh and Singh, 2019; Sood et al., 2012). The gene contains six exons that produce three transcript variants, ILRUNa, ILRUNb and ILRUNc (also referred to as ILRUN-202, ILRUN-203 and ILRUN-201, respectively; Figure 1B & C). ILRUNa and ILRUNb encode for proteins of the same name, ILRUNa (which we will refer to as simply ILRUN) is the full-length protein while ILRUNb is shorter due to loss of exon 4 in the transcript. ILRUNa and ILRUNb both lack the non-protein encoding exon 2 and exon 1 is additionally truncated at the 5' end of ILRUNa, resulting in a shorter 5' UTR compared to ILRUNb. ILRUNc lacks exon 1 and the majority of the 3' UTR encoded by exon 6, but contains exon 2, resulting in a distinct 5' UTR to ILRUNa and ILRUNb.

3.2. ILRUN is widely expressed and appears most abundant in testis and activated B-cells

To gain further insights into the biological functions of ILRUN we performed expression analysis from publicly-available published transcriptomics data (Blischak et al., 2017; Chhibber et al., 2017; Clark et al., 2015; Hipp et al., 2017; Jégou et al., 2017; Kornienko et al., 2016; Lam et al., 2019; Muraro et al., 2016; Nance et al., 2014; Pai et al., 2016; Quinn et al., 2015; Rutering et al., 2016; SEQC/MAQC-III Consortium, 2014; Theurich et al., 2017; Trimarchi et al., 2014; Vecchio et al., 2018; Venken et al., 2019; Wenric et al., 2017; Yu et al., 2015) to investigate the apparent expression of ILRUN transcripts in different human tissues (Figure 2A). ILRUNa transcripts could be detected in all tissues examined, though only very low expression could be detected in spleen and pancreas. Highest abundance was detected in the testis, followed by heart, ovary and adipose. ILRUNb transcripts followed a similar pattern to that of ILRUNa, but were globally much less abundant, with the highest expression detected in the heart and adipose. ILRUNc transcript expression was very low in most tissues, apart from testis and ovary.

Due to the immunological functions of ILRUN (Ambrose et al., 2018), we also investigated its expression in different immune cell populations (Figure 2B). Highest expression of ILRUNa transcripts appeared to be in

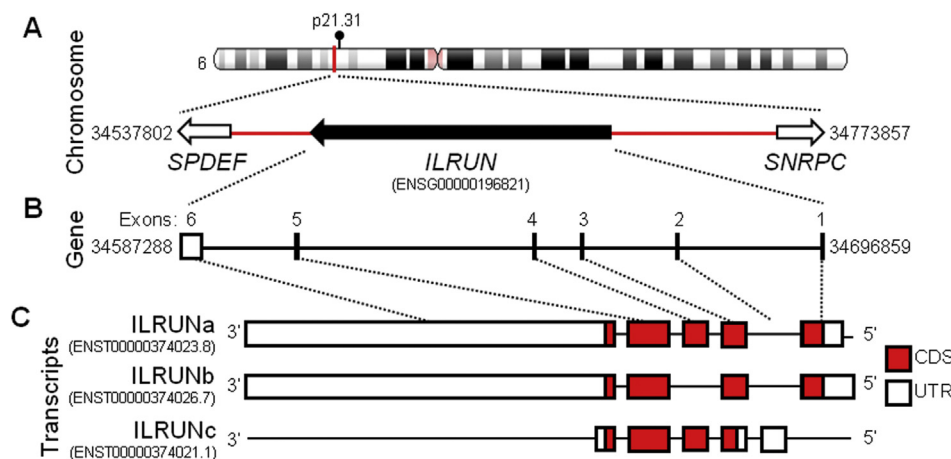


Figure 1. Genomic organisation of the human *ILRUN* locus. (A) Schematic of the human *ILRUN* gene mapped to chromosome 6; chromosome image was obtained from the Genome Decoration Page (NCBI). Arrows denote the direction of genes transcription. (B) Intron-exon organisation of the human *ILRUN* gene. (C) Three transcripts are expressed from the *ILRUN* gene; ILRUNa lack exon 2 and exon 1 is 5' terminally truncated, ILRUNb lacks exon 2 and 5 and ILRUNc lacks exon 1 and the majority of exon 6. Protein coding sequences (CDS; red) and untranslated regions (UTR; white) for each transcript are shown.

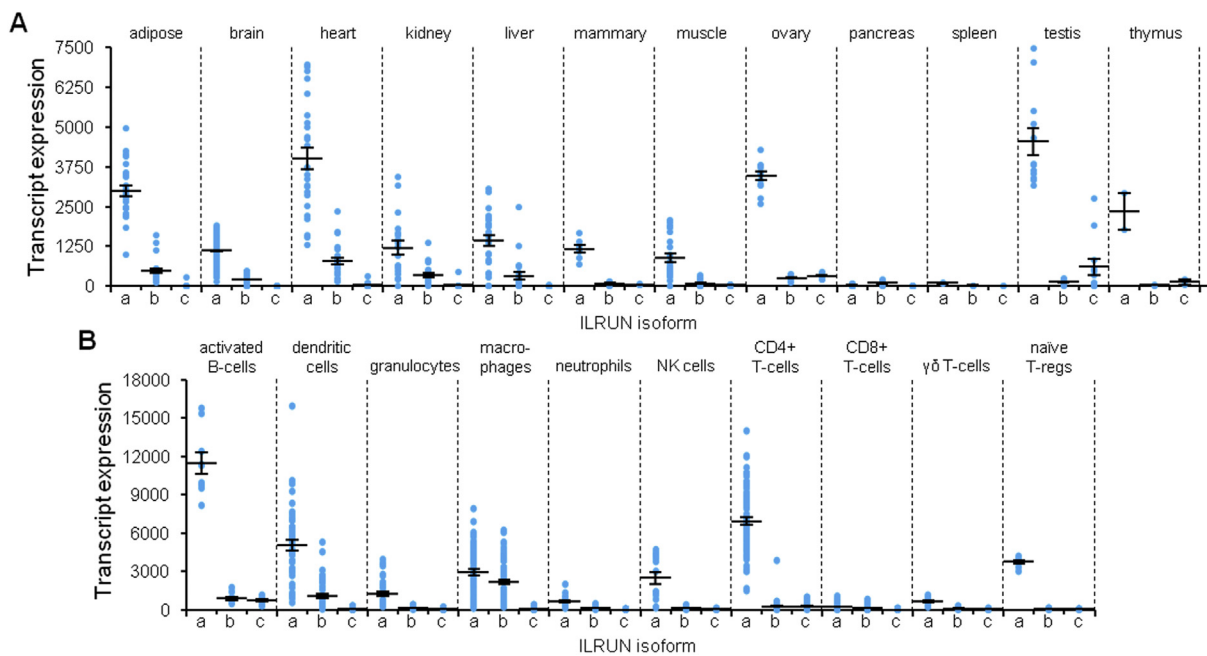


Figure 2. Human ILRUN appears most highly expressed in the testis and activated B-cells. Scatter plots showing expression of *ILRUN* gene transcripts *ILRUNa*, *ILRUNb* and *ILRUNc* in human tissues (A) and immune cells (B). Lines denote the mean (\pm SEM). *ILRUN* expression levels were obtained from peer-reviewed, publicly-available transcriptomics datasets (Blischak et al., 2017; Chhibber et al., 2017; Clark et al., 2015; Hipp et al., 2017; Jégou et al., 2017; Kornienko et al., 2016; Lam et al., 2019; Muraro et al., 2016; Nance et al., 2014; Pai et al., 2016; Quinn et al., 2015; Rutering et al., 2016; SEQC/MAQC-III Consortium, 2014; Theurich et al., 2017; Trimarchi et al., 2014; Vecchio et al., 2018; Venken et al., 2019; Wenric et al., 2017; Yu et al., 2015).

activated B-cells, followed by CD4+ T-cells and dendritic cells. *ILRUNb* was again expressed at much lower level than *ILRUNa* and was most prominent in macrophages. *ILRUNc* was poorly expressed in the cell types examined, except for activated B-cells.

3.3. *ILRUN* is a well-conserved protein that contains UBA-like and NBR1-like domains and a disordered region

ILRUN (accession no. NP_077270.1) is a 298 amino acid protein in humans that is posited to possess a N-terminal UBA-like domain (residues 23–64) and a central NBR1-like domain (residues 71–180; Figure 3A), also referred to as an FW domain due to its four conserved tryptophan residues (Marchbank et al., 2012). The C-terminal region (residues 181–298) is predicted to be largely unstructured (Marchbank et al., 2012), which we have termed the disordered region, and contains three phosphorylation sites at serine residues 215, 222 and 272; these were identified by phosphoproteomic studies (Mayya et al., 2009; Olsen et al.,

2010; Rigbolt et al., 2011; Zhou et al., 2013). The shorter *ILRUNb* isoform (accession no. NP_073595.2) is 232 amino acids, lacking residues 105–170 (Δ 105–170) of the NBR1 domain.

ILRUN orthologues have been identified in nearly all metazoans, with sequence deviation on par with evolutionary divergence (Kriventseva et al., 2019). This is reflected in phylogenetic analysis of *ILRUN* sequences from representative species of different chordate classes, showing stepwise divergence from a common ancestor consistent with their evolutionary distance to humans (Figure 3B). Indeed, *ILRUN* is strongly conserved within this phylum, as amphibian (*Xenopus tropicalis*) *ILRUN* retains 83.6% total protein similarity to that of humans (Figure 3C). *ILRUN* of fish (*Danio rerio*), birds (*Taeniopygia guttata*) and other mammals (*Mus musculus*) show even greater similarity: 87.0%, 93.3% and 96.6%, respectively. Most differences are localised to the disordered domain, which shows a much stronger decline in sequence similarity (91.5% in mice, 88.1% in birds, 73.9% in fish and 52.5% in amphibians) to that of the total protein. This is also associated with a

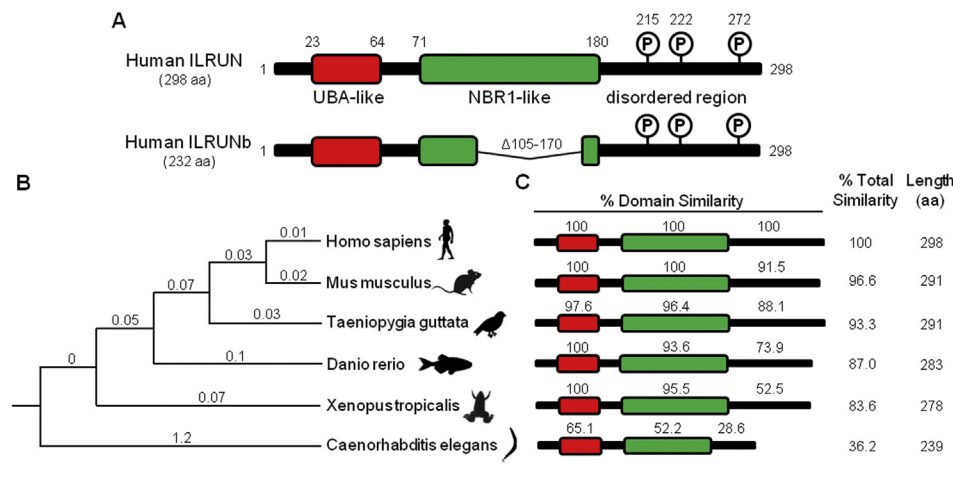


Figure 3. *ILRUN* is a well-conserved protein that contains UBA-like and NBR1-like domains and a disordered region. (A) Predicted protein domain architecture of human *ILRUN* and *ILRUNb*. Numbers represent amino acid positions in full-length *ILRUN*. Putative phosphorylation sites are denoted by an encircled P. (B) Phylogenetic analysis of *ILRUN* genes in different species. A rooted tree was constructed from the amino acid sequences of *ILRUN* using an unweighted pair group method with arithmetic mean using Geneious Prime 2018 version 11.1.4 (Biomatters Ltd.). Numbers indicate number of substitutions per 100 amino acids from a common ancestor. GenBank accession numbers for the respective genes are shown in Supplementary Table A2. (C) Percent amino acid similarity for each domain of *ILRUN* shown in (A), and for full-length protein, from the species listed in (B).

reduction in region length (111 amino acids in mice and birds, 103 in fish and 98 in amphibians, compared to 118 in humans). The UBA-like and NBR1-like domains, on the other hand, are very well-conserved, with a minimum similarity of 97.1% (birds) and 93.6% (fish), respectively.

ILRUN of other phyla appears to be much more diverse, with all domains/regions of nematode ILRUN (*Caenorhabditis elegans*) substantially different to that of humans, 65.1% for the UBA-like domain, 52.5% for the NBR1-like domain and 28.6% for the disordered region. In addition to significant shortening of the disordered domain (52 residues), the size of the NBR1-like domain of nematode ILRUN is also reduced (89 residues compared to 110 in chordates). Despite this divergence, three of the four conserved tryptophan residues of the NBR1-like domain are retained in nematodes, with the forth substituted to a structurally similar phenylalanine residue (Figure 4). Of the three phosphorylation sites identified for ILRUN, S₂₁₅ is the best conserved, present in all chordates but not nematodes, while S₂₂₂ is only present in mammals and S₂₇₂ in mammals and birds (Figure 4).

3.3.1. Crystal structure of the NBR1-like domain and predicted structures of the UBA-like domain of ILRUN

In order to gain insights into the potential function of the domains/regions of ILRUN, we solved the crystal structure of the NBR1-like domain of ILRUN and used QUARK *ab initio* structure prediction software (Xu and Zhang, 2013, 2012) to predict the structure of the UBA-like domain (Figure 5). UBA-like domains are largely involved in binding to ubiquitin and ubiquitin-like (UBL) proteins, which function as post-translational modifiers that target proteins to specific cellular pathways or modify their function (Saeki, 2017). Ubiquitin is 76 amino acid globular protein that is commonly regarded as a marker of proteosomal degradation via conjugation to lysine residues in a target protein by E3 ubiquitin ligases, in association with E1 ubiquitin-activating and E2 ubiquitin-transferring enzymes (Saeki, 2017). As ILRUN promotes the degradation of CBP/p300 (Ambrose et al., 2018), it would seem likely that its UBA-like domain interacts with ubiquitinated CBP/p300 and target them to the proteosome. Prototypical UBA-like domains are three-helix bundles containing a conserved MGF loop between helices 1 and 2 (α 1 and α 2) which is a hydrophobic binding motif that mediates ubiquitin binding (Mueller and Feigon, 2002). Structure prediction suggests that the residues corresponding to the UBA-like domain of ILRUN (residues 23–64) form this bundle (Figure 5A, shown in red); this was confirmed using PDBeFold (EMBL-EBI) structure comparison software, which returned

similarity with existing UBA-like domains (top 10 hits are listed in Supplementary Table A3). Notably, the UBA-like domain of ILRUN contained an LGF motif, though the substitution of leucine for methionine in this motif may not be expected to impact ubiquitin binding as this is also found in the ubiquitin-binding UBA2 domain of the DNA repair protein hHR23A (Wang et al., 2003). In addition, upstream residues of the UBA-like domain may form an additional helix at the N-terminus (α 0) near the UBA-like domain, perhaps forming a non-canonical four-helix UBA-like domain, which has been observed previously in human nuclear RNA export factor (NXF) 1/2 and yeast tyrosyl DNA phosphodiesterase 2 (TDP2) (Grant et al., 2002; Rao et al., 2016).

The central domain of ILRUN is termed NBR1-like due to its homology to the FW domain of NBR1 (Marchbank et al., 2012). At present only NBR1 and ILRUN have been categorised to possess a FW/NBR1-like domain in animals, but it has been identified in several bacterial proteins (Marchbank et al., 2012). Our 2.5 Å crystal structure of the ILRUN NBR1-like domain obtained by limited proteolysis consists of seven antiparallel β -strands arranged in a small β -sandwich (Figure 5B; deposited in the RCSB Protein Data Bank under ID 6VH1; statistics shown in Supplementary Table A4). It adopts a fibronectin type-III topology (Figure 5C) and the location of these β -sheets are similar to previous secondary structure predictions of the FW domains of ILRUN and NBR1 from several different species, which proposed a six β -sheet domain, lacking β 4 (Marchbank et al., 2012). Three of the four conserved tryptophans (W₉₉, W₁₀₉ and W₁₅₉) are buried in the hydrophobic core of the domain whereas the fourth (W₁₇₄) is solvent exposed (Figure 5B).

3.4. Both the UBA-like and NBR1-like domains of ILRUN are necessary for inhibition of IRF3-dependent DNA-binding and induction of IFN β gene expression, while the disordered region appears dispensable

To evaluate the contributions of each of the domains of ILRUN to its function in inhibiting IRF3-dependent IFN β gene expression, we generated three mutant constructs containing deletions of each domain (Figure 6A). Δ UBA contains deletion of residues 1–74, removing the UBA-like domain and all residues upstream of the NBR1-like domain, corresponding to the predicted protein sequence encoded by ILRUNc. Δ NBR1 is homologous in sequence to ILRUNb, lacking residues 105–170 of the NBR1-like domain. Finally, we truncated the disordered domain at residue 193 (Δ dis) to not impact a hydrophobic patch that may constitute a possible transmembrane domain (not shown).

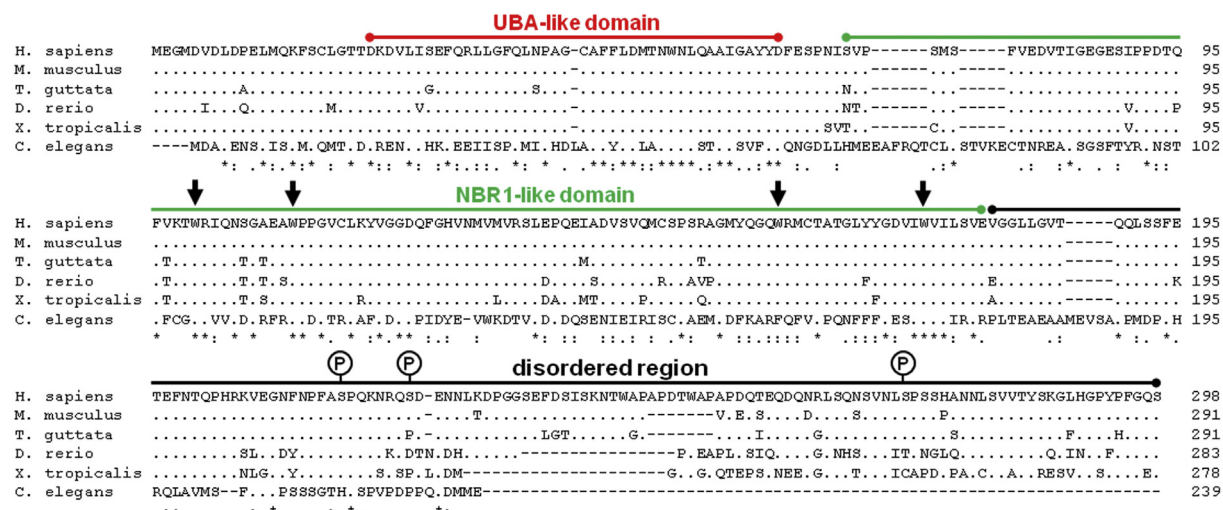


Figure 4. Multiple alignment of human ILRUN with orthologues from other species. Multiple sequence alignments of ILRUN proteins from different species were performed using Clustal Omega (European Bioinformatics Institute). Identical (*), conserved (:), and semi-conserved (.) residues are denoted below the sequences. Arrows indicate key tryptophan (W) residues of the NBR1 domain and putative phosphorylation sites are denoted by an encircled P.

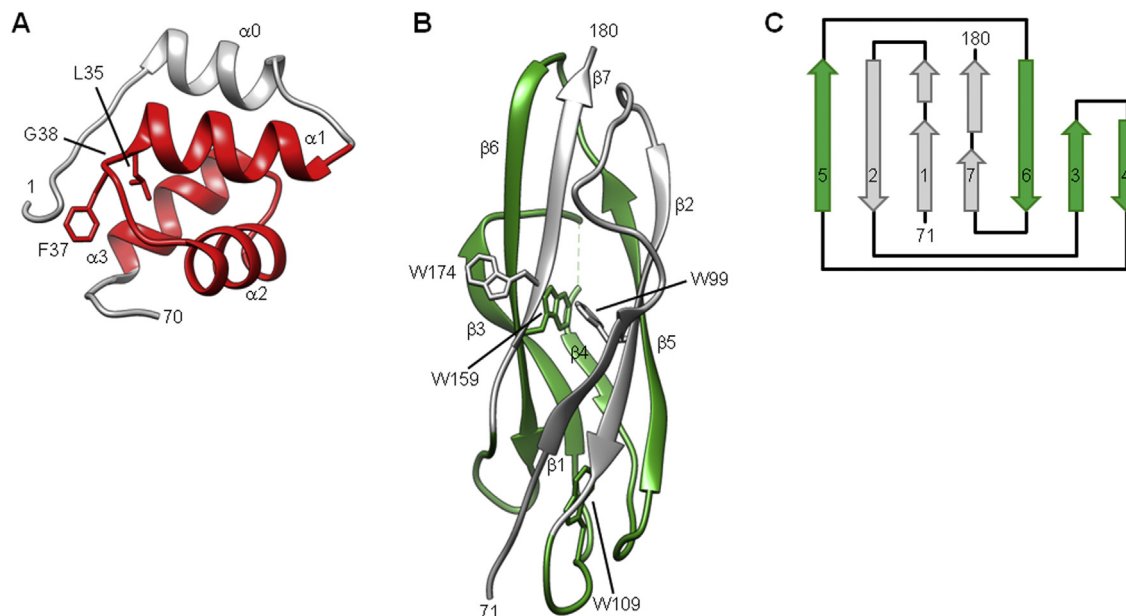


Figure 5. Modelling of UBA-like domain and structural determination of NBR1-like domain of ILRUN. (A) Ribbon diagram of a structure prediction of residues 1–70 of ILRUN, including the predicted UBA-like domain (residues 23–64, shown in red), using QUARK *ab initio* structure prediction software (Xu and Zhang, 2013, 2012). Secondary structure and predicted ubiquitin-binding (LGF) motif are indicated. (B) Ribbon diagram of a 2.5 Å crystal structure of the ILRUN NBR1-like domain obtained by limited proteolysis. Secondary structure and conserved tryptophan (W) residues are indicated, and sequences not present in ILRUNb (residues 105–170) are shown in green. (C) 2D schematic of the ribbon diagram shown in (B). Graphics in (A) and (B) were generated using UCSF Chimera (Pettersen et al., 2004).

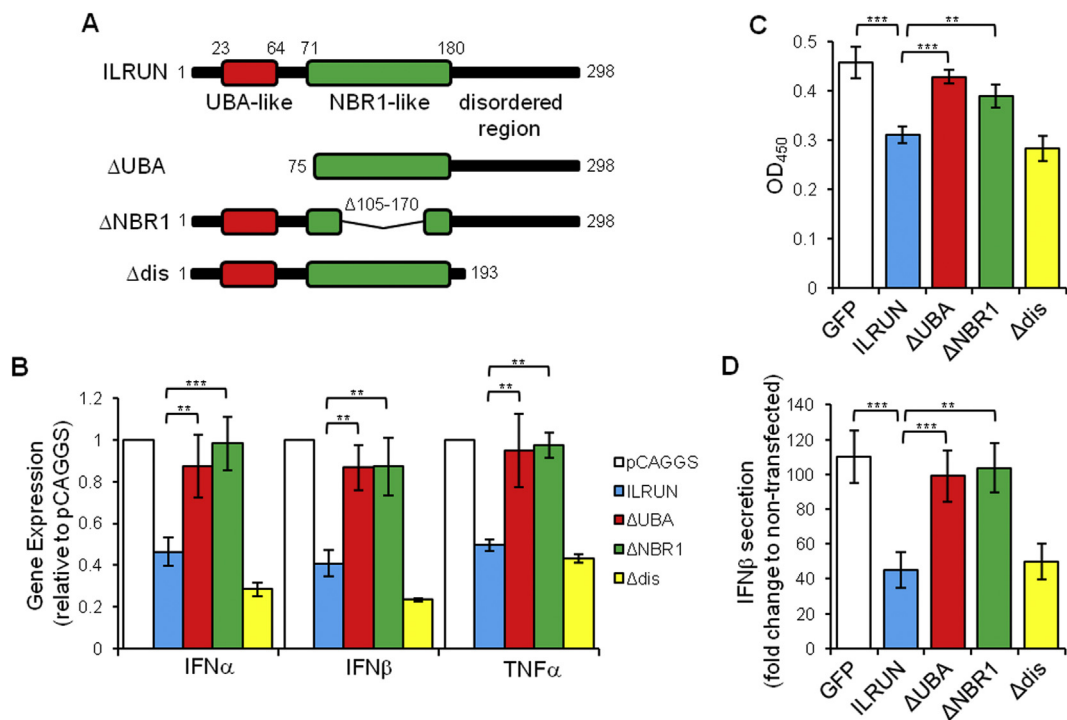


Figure 6. Both the UBA-like and NBR1-like domains of ILRUN are necessary for inhibition of IRF3 signalling, while the disordered region is dispensable. (A) Schematic of ILRUN mutants, including wild-type ILRUN, ΔUBA, lacking residues 1–75, ΔNBR1, lacking residues 105–170, and Δdis, lacking residues 194–298. (B) HeLa cells were transfected with plasmids expressing the indicated proteins (or empty vector/pCAGGS) for 24 h before treatment with transfected poly(I:C) (5 µg/mL) for 6 h, with cells collected and analyzed for mRNA expression of the listed cytokines by qRT-PCR. (C) HeLa cells were transfected with plasmids expressing the indicated proteins and stimulated with poly(I:C), and the nuclear proteins were extracted using a hypotonic lysis method. Nuclear proteins (10 µg) were analyzed for IRF3–DNA binding. (D) Cell supernatants from cells used in (C) were analyzed for IFN-β protein by ELISA assay. Error bars denote ±SEM of three independent experiments, and asterisks show significant changes compared with controls as measured by one- or two-way ANOVA with Bonferroni post-test (***, $p < 0.001$; **, $p < 0.01$).

These mutant constructs, in addition to full-length ILRUN and a negative control expressing GFP or empty vector (pCAGGS), were transfected into HeLa cells, stimulated with poly(I:C) (5 µg/mL, 6 h), and IRF3-DNA binding assessed using an IRF3 transcription factor kit (abcam; Figure 6C). IFN β mRNA and protein expression were also quantified by qRT-PCR (Figure 6B) and ELISA (Figure 6D), respectively. Over-expression of wild-type ILRUN inhibited IRF3 signalling, as expected (Ambrose et al., 2018), marked by a reduction in IRF3-DNA binding (Figure 6B), IFN β secretion (Figure 6D) and transcription of IFN α , IFN β and TNF α transcription (Figure 6C) compared to controls. The deletion of either the UBA-like (Δ UBA) or NBR1-like (Δ NBR1) domains abrogated the functional activity of ILRUN across all assays employed, indicating both these domains are necessary to inhibit IRF3 signalling. Deletion of the disordered domain (Δ dis) did not appear to have an impact on ILRUN function in these assays.

4. Discussion

The type I IFNs are critical regulators of the antiviral immune response, inducing an antiviral state via production of interferon-stimulated genes (ISGs), upregulating major histocompatibility complex expression to promote lysis of infected cells, and triggering further cytokine and chemokine expression to recruit immune cells to fight infection (Stetson and Medzhitov, 2006). Type I IFNs also promote differentiation and maturation of dendritic and natural killer cells and perform both positive and negative regulatory roles in adaptive immune responses to infection (Dauer et al., 2003; McNab et al., 2015; Swann et al., 2007). Through the sharing or redundancy of signalling pathways, type-I IFN production is often accompanied by the production of pro-inflammatory cytokines, including IL-6 and TNF α , which stimulate acute phase responses, hematopoiesis, and further immune activation (Tanaka et al., 2014). Whilst these cytokines are essential for antimicrobial defence, aberrant regulation of their synthesis results in autoimmune diseases including rheumatoid arthritis, lupus and systemic sclerosis (Stetson and Medzhitov, 2006). Excessive proinflammatory responses can also lead to fatal ‘cytokine storm’ associated with severe viral infection (Liu et al., 2016; Srikiatkachorn et al., 2017; Younan et al., 2017). Furthermore, sustained IFN production can cause alterations to the epigenetic landscape through chromatin remodelling, altering the scale of inflammatory responses resulting from immune stimulation (Kamada et al., 2018; Park et al., 2017). Effective regulation of cytokine production is therefore essential in the homeostasis between health and disease. Thus, our recent characterisation of ILRUN as an inhibitor of type-I IFNs and TNF α adds another component to this network, likely working in concert with other negative regulators of cytokine transcription, such as IL-37, sterile alpha motif and HD-domain-containing protein 1 (SAMHD1) and HLA-F adjacent transcript 10 (FAT10), which target various stages of the IFN induction pathway (Ambrose et al., 2018; Chen et al., 2018; Gallenga et al., 2019; Nguyen et al., 2016).

Unlike other cytokine inhibitors, however, ILRUN features an uncommon mechanism of action whereby IRF3-dependent transcription of these cytokines is blocked without impacting IRF3 activation, nuclear translocation or degradation (Ambrose et al., 2018). Instead, ILRUN appears to carry out this function by inducing the degradation of the transcriptional co-activators CBP/p300, which participate in the transcription of the *IFN β* gene as part of the IFN β enhanceosome complex (Ambrose et al., 2018). In the present study we demonstrate that the highly conserved UBA-like and NBR1-like domains of ILRUN are essential for its regulation of IFN production. To our knowledge, the only cellular protein comparable to ILRUN from a mechanistic perspective is cFLIPL (cellular FLICE-like inhibitory protein, long isoform), which shares no molecular homology with ILRUN but binds IRF3 to inhibit interactions between the transcriptional coactivator CBP and the IFN β promoter (Gates and Shisler, 2016). Interestingly, cFLIPL also inhibits IRF7-dependent IFN α transcription by binding I κ B kinase- α (IKK α) and preventing IKK α from phosphorylating and activating IRF7

(Gates-Tanzer and Shisler, 2018). The effect of ILRUN on steady-state CBP/p300 protein levels raises the possibility that, similar to cFLIPL, ILRUN regulates IFN signalling more broadly than only via IRF3.

Our expression analysis of ILRUN transcript expression in different human tissues revealed the highest abundance of ILRUNA in testis, heart, ovary and adipose. Small nucleotide polymorphisms (SNPs) in the *ILRUN* gene have been associated with increased risk of obesity (Ahmad et al., 2016; Baranski et al., 2018; Riveros-McKay et al., 2019), therefore high levels of ILRUN in adipose may not be surprising. Expression in the testis and ovary may relate to the unique innate immune environment of these organs due to the need to avoid autoimmunity against gametes, preventing chronic inflammation that can lead to infertility and, in the case of the female reproductive tract (FRT), ensure tolerance to semen and the fetus (Cumming and Bourke, 2019; Mossadegh-Keller and Sieweke, 2018). The FRT also constitutively expresses IFNe, a type-I IFN whose expression is highly restricted to the mucosal epithelium of the gut, lung, brain and FRT (Cumming and Bourke, 2019). Strong expression of IFNe transcripts have also been detected in the testes of mice compared to other tissues (Hermant et al., 2013). Thus, ILRUN may have integral roles in maintaining immune homeostasis of reproductive organs. Furthermore, male germ cells are enriched in mRNA transcripts that undergo distinct splicing events to somatic cells, including truncation of 3' UTRs (Berkovits et al., 2012; McMahon et al., 2006; Wang et al., 2006), consistent with the highest expression of the ILRUNc transcript, which lacks most of the 3' UTR present in ILRUNA and ILRUNb, occurring in testis. This may allude to potential functions of this isoform, and perhaps full-length ILRUN as well, in spermatogenesis if it is, in fact, translated into protein. Finally, aberrant IFN/IRF3 signalling is particularly detrimental to the heart, likely requiring strong inhibitory mechanisms to prevent tissue damage (King et al., 2017), which may be mediated by ILRUN.

This analysis also showed an apparent abundance of ILRUNA transcripts in activated B-cells, CD4+ T-cells and macrophages. Prolonged type-I IFN signalling is detrimental to B- and T-cell function, leading to suppression of CD4+ T-cell function and generation of autoantibodies by B-cells (Cervantes-Luevano et al., 2018; Lee et al., 2016; Nguyen et al., 2015; Osokine et al., 2014; Snell et al., 2017; Xu et al., 2018). Thus, ILRUN may serve to temper IFN production by these cell types to prevent immune dysregulation. Dendritic cells, especially plasmacytoid dendritic cells, are professional type-I IFN producers (Sweicki and Colonna, 2015), therefore high levels of ILRUN may be necessary for shutting down the strong expression of type-I IFNs during infection by these cells following pathogen clearance.

Our investigation of the contributions of the domains of ILRUN to its ability to inhibit IRF3 signalling determined that both the UBA-like and NBR1-like domains are important. UBA-like domains are largely involved in binding to ubiquitin and targeting ubiquitinated proteins to the proteasome for degradation (Saeki, 2017); this would appear to be the likely function of this domain in ILRUN, enabling association to ubiquitinated CBP/p300 and promoting its degradation. However, both ubiquitin and UBA-like domains have additional diverse functions. Ubiquitin is also involved in DNA damage responses, cell cycle regulation, protein trafficking, signal transduction and protein scaffolding, dependent on the number and chain configuration of the ubiquitin tag (Swatek and Komander, 2016). UBA-like domains also mediate association with ULPs that are structurally similar to ubiquitin and are involved in various cellular processes (van der Veen and Ploegh, 2012). In relation to ILRUN, two ULPs of note are small ubiquitin-related modifier (SUMO), which has roles in gene transcription, and IFN-stimulated gene 15 (ISG15), which has antiviral functions (van der Veen and Ploegh, 2012). Thus, the UBA-like domain of ILRUN has the potential to be multifunctional, enabling modulation multiple cellular processes.

FW/NBR1-like domains have been previously proposed to mediate homo- or heterodimerisation and/or associate with small molecules (Marchbank et al., 2012). While the function of the FW domain of NBR1 still remains to be completely elucidated, studies have shown that this

region interacts with the light chain of MAP1B, potentially to enable association with the microtubule cytoskeleton, a cellular structure with integral roles in autophagy (Marchbank et al., 2012), suggesting that the ILRUN NBR1-like domain could be involved in mediating protein-protein interactions. Furthermore, truncations encompassing this domain in NBR1 contribute to its localisation to late endosomes and its ability to inhibit ligand-mediated receptor tyrosine kinase degradation (Mardakheh et al., 2010).

The C-terminal region of ILRUN is predicted to be largely disordered (Marchbank et al., 2012), and our data suggests it does not contribute to antagonism of IRF3 signalling. However, intrinsically disordered regions (IDRs), regions of proteins that lack stable tertiary structure under physiological conditions, can provide great diversity to protein function by providing a means to potentially adopt multiple conformations in a regulated manner, enabling a single protein to effect diverse outcomes dependent on interactions with different ligands/proteins (Tompa et al., 2015; Wright and Dyson, 2015). IDRs are also regulated by post-translational modifications (Bah and Forman-Kay, 2016), suggesting that the three phosphorylation sites identified in the disordered region of ILRUN may regulate its conformation/function. Thus, the lack of conservation of these sites in different species may indicate different modes of regulation. While the functions of IDRs are broad, RNA-binding proteins and transcriptions factors in particular are enriched for IDRs, indicating importance in regulating gene expression (Basu and Bahadur, 2016; Skupien-Rabian et al., 2016).

Whilst our work implicates ILRUN in antiviral immunity, other studies point to broader biological roles (summarised briefly in Supplementary Table A5). The role of ILRUN in inflammatory signalling, described by our group, in addition to unpublished findings relating to lipid metabolism (Bi et al., 2020), form the basis for the name ILRUN. Roles in lipid metabolism may be associated with genome-wide SNP studies implicating ILRUN in obesity (Ahmad et al., 2016; LeBlanc et al., 2016; Locke et al., 2015; Riveros-McKay et al., 2019). These studies additionally suggest roles for ILRUN in height, the timing of pubescent growth spurts and coronary heart disease (LeBlanc et al., 2016; Lee et al., 2010; Sovio et al., 2009; Zhao et al., 2010). In the context of cancer, increased expression of ILRUN mRNA and protein have been described in pancreatic, breast and non-small cell lung cancer (NSCLC) tissue, where expression positively correlates with poor NSCLC prognosis (Jiang et al., 2015; Li et al., 2019; Zhang et al., 2015). In pancreatic cancer tissue, overexpression of ILRUN increases cell proliferation and cancer cell invasion, possibly through stimulation of the ERK-P90RSK signalling pathway (Li et al., 2019). Additionally, due to the anti-cancer functions of type-I IFNs and TNF α (Shen et al., 2018; Zitvogel et al., 2015), inhibition of these cytokines by ILRUN would likely also contribute to these apparent oncogenic effects.

An interesting hypothesis for future research is that, in addition to its regulation of type-I IFN and TNF α expression, ILRUN is linked to these diseases via its effect on the transcriptional coactivator proteins CBP/p300. We have shown that ILRUN reduces nuclear levels of CBP/p300 without impacting their expression in the cytoplasm (Ambrose et al., 2018). These proteins are histone acetyltransferase (HAT) enzymes that catalyse the acetylation of lysine residues within promoter-bound histones, resulting in chromatin relaxation and modulation of transcription (Chan and La Thangue, 2001). CBP/p300 interact with over 300 different cellular and viral binding partners to regulate physiological events including proliferation, differentiation, infection and apoptosis, among others (Chan and La Thangue, 2001). Dysregulation of epigenetic modifications is associated with the pathology of many diseases, including coronary artery disease and cancer (Iyer et al., 2004; Wang et al., 2013). Indeed, the domain composition of ILRUN could certainly suggest specific functions in transcription regulation, beyond simply acting as a ‘chaperone’ for CBP/p300 degradation. Together, the data presented here and the nominal literature available for ILRUN suggest it may have many functions/modes of action that impact on a number of cellular processes relevant to disease.

5. Conclusions

In summary, ILRUN is a highly conserved regulator proinflammatory and antiviral cytokines, with its UBA-like and NBR1-like domains essential for this function. Expression of ILRUN transcripts is observed in all tissues and immune cell types examined and appears most highly expressed in testis and activated B-cells. Further work will be required to understand the mechanism by which ILRUN regulates inflammation and antiviral responses through its effects on CBP/p300 expression and to explore other potential biological functions for this protein.

Declarations

Author contribution statement

R. Ambrose: Conceived and designed the experiments; Performed the experiments; Analyzed and interpreted the data; Contributed reagents, materials, analysis tools or data.

A. Brice: Analyzed and interpreted the data; Contributed reagents, materials, analysis tools or data; Wrote the paper.

A. Caputo and C. Stewart: Conceived and designed the experiments; Performed the experiments; Analyzed and interpreted the data; Contributed reagents, materials, analysis tools or data; Wrote the paper.

M. Alexander, Y. Liu and L. Tribolet: Performed the experiments; Analyzed and interpreted the data; Contributed reagents, materials, analysis tools or data.

T. Adams and A. Bean: Conceived and designed the experiments; Analyzed and interpreted the data; Contributed reagents, materials, analysis tools or data.

Funding statement

C. Stewart, A. Bean and T. Adams were supported by CSIRO postdoctoral fellowships.

Competing interest statement

The authors declare no conflict of interest.

Additional information

Supplementary content related to this article has been published online at <https://doi.org/10.1016/j.heliyon.2020.e04115>.

Acknowledgements

All crystallisation experiments were carried out at the CSIRO Collaborative Crystallisation Centre (www.csiro.au/C3), Melbourne, Australia. This research was undertaken in part using the MX2 beamline at the Australian Synchrotron, part of ANSTO, and made use of the Australian Cancer Research Foundation (ACRF) detector. Molecular graphics were generated with UCSF Chimera, developed by the Resource for Biocomputing, Visualization, and Informatics at the University of California, San Francisco, with support from NIH P41-GM103311.

References

- Marchbank, K., Waters, S., Roberts, R.G., Solomon, E., Whitehouse, C.A., 2012. MAP1B interaction with the FW domain of the autophagic receptor Nbr1 facilitates its association to the microtubule network. *Int. J. Cell Biol.* 2012, 1–11.
- Ahmad, S., Poveda, A., Shungin, D., Barroso, I., Hallmans, G., Renström, F., Franks, P.W., 2016. Established BMI-associated genetic variants and their prospective associations with BMI and other cardiometabolic traits: the GLACIER Study. *Int. J. Obes.* 40, 1346–1352.
- Ambrose, R.L., Liu, Y.C., Adams, T.E., Bean, A.G.D., Stewart, C.R., 2018. C6orf106 is a novel inhibitor of the interferon-regulatory factor 3-dependent innate antiviral response. *J. Biol. Chem.* 293, 10561–10573.

- Bah, A., Forman-Kay, J.D., 2016. Modulation of intrinsically disordered protein function by post-translational modifications. *J. Biol. Chem.* 291, 6696–6705.
- Baranski, T.J., Kraja, A.T., Fink, J.L., Feitosa, M., Lenzini, P.A., Borecki, I.B., Liu, C.-T., Cupples, L.A., North, K.E., Province, M.A., 2018. A high throughput, functional screen of human Body Mass Index GWAS loci using tissue-specific RNAi *Drosophila melanogaster* crosses. *PLOS Genet* 14, e1007222.
- Basu, S., Bahadur, R.P., 2016. A structural perspective of RNA recognition by intrinsically disordered proteins. *Cell. Mol. Life Sci.* 73, 4075–4084.
- Berkovits, B.D., Wang, L., Guarneri, P., Wolgemuth, D.J., 2012. The testis-specific double bromodomain-containing protein BRDT forms a complex with multiple spliceosome components and is required for mRNA splicing and 30-UTR truncation in round spermatids. *Nucleic Acids Res.* 40, 7162–7175.
- Bi, X., Kuwano, T., Lee, P., Millar, J.S., Soccio, R., Hand, N.J., Rader, D.J., 2020. Abstract 13712: ILRUN, A novel plasma lipid and CAD locus in humans, regulates lipoprotein metabolism and atherogenesis in mice. In: American Heart Association's 2019 Scientific Sessions.
- Blischak, J.D., Tailleux, L., Myrthil, M., Charlois, C., Bergot, E., Dinh, A., Morizot, G., Chény, O., Platen, C., Von, Herrmann, J.L., Brosch, R., Barreiro, L.B., Gilad, Y., 2017. Predicting susceptibility to tuberculosis based on gene expression profiling in dendritic cells. *Sci. Rep.* 7, 1–11.
- Bricogne, G., Blanc, E., Brandl, M., Flensburg, C., Keller, P., Paciorek, W., Roversi, P., Sharff, A., Smart, O.S., Vonrhein, C., Womack, T.O., 2017. BUSTER Version 2.10.3. Cervantes-Luevano, K.E., Caronni, N., Castiello, M.C., Fontana, E., Piperno, G.M., Naseem, A., Uva, P., Bosticardo, M., Marcovecchio, G.E., Notarangelo, L.D., Cicalese, M.P., Aiuti, A., Villa, A., Benvenuti, F., 2018. Neutrophils drive type I interferon production and autoantibodies in patients with Wiskott-Aldrich syndrome. *J. Allergy Clin. Immunol.* 142, 1605–1617 e4.
- Chan, H.M., La Thangue, N.B., 2001. p300/CBP proteins: HATs for transcriptional bridges and scaffolds. *J. Cell Sci.* 114, 2363–2373.
- Chen, K., Liu, J., Cao, X., 2017. Regulation of type I interferon signaling in immunity and inflammation: a comprehensive review. *J. Autoimmun.* 83, 1–11.
- Chen, S., Bonifati, S., Qin, Z., Gelais, C.S., Kodigepalli, K.M., Barrett, B.S., Kim, S.H., Antonucci, J.M., Ladner, K.J., Buzovetsky, O., Knecht, K.M., Xiong, Y., Yount, J.S., Guttridge, D.C., Santiago, M.L., Wu, L., 2018. SAMHD1 suppresses innate immune responses to viral infections and inflammatory stimuli by inhibiting the NF- κ B and interferon pathways. *Proc. Natl. Acad. Sci. U. S. A.* 115, E3798–E3807.
- Chhibber, A., French, C.E., Yee, S.W., Gamazon, E.R., Theusch, E., Qin, X., Webb, A., Papp, A.C., Wang, A., Simmons, C.Q., Konkashbaev, A., Chaudhry, A.S., Mitchel, K., Stryke, D., Ferrin, T.E., Weiss, S.T., Kroetz, D.L., Sadee, W., Nickerson, D.A., Krauss, R.M., George, A.I., Schuetz, E.G., Medina, M.W., Cox, N.J., Scherer, S.E., Giacomini, K.M., Brenner, S.E., 2017. Transcriptomic variation of pharmacogenes in multiple human tissues and lymphoblastoid cell lines. *Pharmacogenomics J.* 17, 137–145.
- Clark, M.B., Mercer, T.R., Bussotti, G., Leonardi, T., Haynes, K.R., Crawford, J., Brunck, M.E., Cao, K.-A.L., Thomas, G.P., Chen, W.Y., Taft, R.J., Nielsen, L.K., Enright, A.J., Mattick, J.S., Dinger, M.E., 2015. Quantitative gene profiling of long noncoding RNAs with targeted RNA sequencing. *Nat. Methods* 12, 339–342.
- Cumming, H.E., Bourke, N.M., 2019. Type I IFNs in the female reproductive tract: the first line of defense in an ever-changing battleground. *J. Leukoc. Biol.* 105, 353–361.
- Dauer, M., Pohl, K., Obermaier, B., Meskendahl, T., Röbe, J., Schnurr, M., Endres, S., Eigler, A., 2003. Interferon- α disables dendritic cell precursors: dendritic cells derived from interferon- α -treated monocytes are defective in maturation and T-cell stimulation. *Immunology* 110, 38–47.
- Fuertes, M.B., Woo, S.-R., Burnett, B., Fu, Y.-X., Gajewski, T.F., 2013. Type I interferon response and innate immune sensing of cancer. *Trends Immunol.* 34, 67–73.
- Gallenga, C.E., Pandolfi, F., Caraffa, A., Kritas, S.K., Ronconi, G., Toniato, E., Martinotti, S., Conti, P., 2019. Interleukin-1 family cytokines and mast cells: activation and inhibition. *J. Biol. Regul. Homeost. Agents* 33, 1–6.
- Gates, L.T., Shisler, J.L., 2016. cFLIP L interrupts IRF3-CBP-DNA interactions to inhibit IRF3-driven transcription. *J. Immunol.* 197, 923–933.
- Gates-Tanzer, L.T., Shisler, J.L., 2018. Cellular FLIP long isoform (cFLIP L)-IKK α interactions inhibit IRF7 activation, representing a new cellular strategy to inhibit IFN α expression. *J. Biol. Chem.* 293, 1745–1755.
- Grant, R.P., Hurt, E., Neuhaus, D., Stewart, M., 2002. Structure of the C-terminal FG-nucleoporin binding domain of Tap/NXF1. *Nat. Struct. Biol.* 9, 247–251.
- Herman, P., Francius, C., Clotman, F., Michiels, T., 2013. IFN- ϵ is constitutively expressed by cells of the reproductive tract and is inefficiently secreted by fibroblasts and cell lines. *PLoS One* 8, 1–9.
- Hipp, N., Symington, H., Pastoret, C., Caron, G., Monvoisin, C., Tarte, K., Fest, T., Delaloy, C., 2017. IL-2 imprints human naïve B cell fate towards plasma cell through ERK/ELK1-mediated BACH2 repression. *Nat. Commun.* 8.
- Iyer, N.G., Özdag, H., Caldas, C., 2004. p300/CBP and cancer. *Oncogene* 23, 4225–4231.
- Jégou, B., Sankararaman, S., Rolland, A.D., Reich, D., Chalmel, F., 2017. Meiotic genes are enriched in regions of reduced archaic ancestry. *Mol. Biol. Evol.* 34, 1974–1980.
- Jiang, G., Zhang, X., Zhang, Y., Wang, L., Fan, C., Xu, H., Miao, Y., Wang, E., 2015. A novel biomarker C6orf106 promotes the malignant progression of breast cancer. *Tumor Biol.* 36, 7881–7889.
- Kabsch, W., 2010. XDS. *Acta Crystallogr. D. Biol. Crystallogr.* 66, 125–132.
- Kamada, R., Yang, W., Zhang, Y., Patel, M.C., Yang, Y., Ouda, R., Dey, A., Wakabayashi, Y., Sakaguchi, K., Fujita, T., Tamura, T., Zhu, J., Ozato, K., 2018. Interferon stimulation creates chromatin marks and establishes transcriptional memory. *Proc. Natl. Acad. Sci. U. S. A.* 115, E9162–E9171.
- King, K.R., Aguirre, A.D., Ye, Y.-X., Sun, Y., Roh, J.D., Ng, R.P., Kohler, R.H., Arlauckas, S.P., Iwamoto, Y., Savol, A., Sadreyev, R.I., Kelly, M., Fitzgibbons, T.P., Fitzgerald, K.A., Mitchison, T., Libby, P., Nahrendorf, M., Weissleder, R., 2017. IRF3 and type I interferons fuel a fatal response to myocardial infarction. *Nat. Med.* 23, 1481–1487.
- Kornienko, A.E., Dotter, C.P., Guenzl, P.M., Gisslinger, H., Gisslinger, B., Cleary, C., Kralovics, R., Paurer, F.M., Barlow, D.P., 2016. Long non-coding RNAs display higher natural expression variation than protein-coding genes in healthy humans. *Genome Biol.* 17, 1–23.
- Kriventseva, E.V., Kuznetsov, D., Tegenfeldt, F., Manni, M., Dias, R., Simão, F.A., Zdobnov, E.M., 2019. OrthoDB v10: sampling the diversity of animal, plant, fungal, protist, bacterial and viral genomes for evolutionary and functional annotations of orthologs. *Nucleic Acids Res.* 47, D807–D811.
- Lachmann, A., Torre, D., Keenan, A.B., Jagodnik, K.M., Lee, H.J., Wang, L., Silverstein, M.C., Ma'ayan, A., 2018. Massive mining of publicly available RNA-seq data from human and mouse. *Nat. Commun.* 9, 1366.
- Lam, A.J., MacDonald, K.N., Pesenacker, A.M., Juvet, S.C., Morishita, K.A., Bressler, B., iGenoMed Consortium, Pan, J.G., Sidhu, S.S., Rioux, J.D., Levings, M.K., 2019. Innate control of tissue-reparative human regulatory T cells. *J. Immunol.* 202, 2195–2209.
- LeBlanc, M., Zuber, V., Andreassen, B.K., Witoelar, A., Zeng, L., Bettella, F., Wang, Y., McEvoy, L.K., Thompson, W.K., Schork, A.J., Reppe, S., Barrett-Connor, E., Ligthart, S., Dehghan, A., Gautvik, K.M., Nelson, C.P., Schunkert, H., Samani, N.J., CARDIoGRAM Consortium, Ridker, P.M., Chasman, D.I., Aukrust, P., Djurovic, S., Frigessi, A., Desikan, R.S., Dale, A.M., Andreassen, O.A., 2016. Identifying novel gene variants in coronary artery disease and shared genes with several cardiovascular risk factors. *Circ. Res.* 118, 83–94.
- Lee, J.J., Essers, J.B., Kugathasan, S., Escher, J.C., Lettre, G., Butler, J.L., Stephens, M.C., Ramoni, M.F., Grand, R.J., Hirschhorn, J., 2010. Association of linear growth impairment in pediatric Crohn's disease and a known height locus: a pilot study. *Ann. Hum. Genet.* 74, 489–497.
- Lee, B.R., Jeong, S.K., Ahn, B.C., Lee, B.J., Shin, S.J., Yum, J.S., Ha, S.J., 2016. Combination of TLR1/2 and TLR3 ligands enhances CD4+ T cell longevity and antibody responses by modulating type I IFN production. *Sci. Rep.* 6, 1–11.
- Li, X., Dong, M., Zhou, J., Zhu, D., Zhao, J., Sheng, W., 2019. C6orf106 accelerates pancreatic cancer cell invasion and proliferation via activating ERK signaling pathway. *Mol. Cell. Biochem.* 454, 87–95.
- Liu, Q., Zhou, Y., Yang, Z., 2016. The cytokine storm of severe influenza and development of immunomodulatory therapy. *Cell. Mol. Immunol.* 13, 3–10.
- Locke, A.E., Kahali, B., Berndt, S.I., Justice, A.E., Pers, T.H., Day, F.R., Powell, C., Vedantam, S., Buchkovich, M.L., Yang, J., Croteau-Chonka, D.C., Esko, T., Fall, T., Ferreira, T., Gustafsson, S., Kutalik, Z., Luan, J., Mági, R., Randall, J.C., Winkler, T.W., Wood, A.R., Workalemahu, T., Faul, J.D., Smith, J.A., Zhao, J.H., Zhao, W., Chen, J., Fehrmann, R., Hedman, Å.K., Karjalainen, J., Schmidt, E.M., Absher, D., Amin, N., Anderson, D., Beekman, M., Bolton, J.L., Bragg-Gresham, J.L., Buyske, S., Demirkiran, A., Deng, G., Ehret, G.B., Feenstra, B., Feitosa, M.F., Fischer, K., Goel, A., Gong, J., Jackson, A.U., Kanoni, S., Kleber, M.E., Kristiansson, K., Lim, U., Lotay, V., Mangino, M., Leach, I.M., Medina-Gomez, C., Medland, S.E., Nalls, M.A., Palmer, C.D., Pasko, D., Pechlivanis, S., Peters, M.J., Prokopenko, I., Shungin, D., Stančáková, A., Strawbridge, R.J., Sung, Y.J., Tanaka, Toshiko, Teumer, A., Trompet, S., van der Laan, S.W., van Setten, J., Vliet-Ostaptchouk, J.V., Van, Wang, Z., Yengo, L., Zhang, W., Isaacs, A., Albrecht, E., Årnlöv, J., Arscott, G.M., Attwood, A.P., Bandinelli, S., Barrett, A., Bas, I.N., Bellis, C., Bennett, A.J., Berne, C., Blagieva, R., Blüher, M., Börhringer, S., Bonnycastle, L.L., Böttcher, Y., Boyd, H.A., Bruinenberg, M., Caspersen, I.H., Chen, Y.-D.I., Clarke, R., Daw, E.W., de Craen, A.J.M., Delgado, G., Dimitriou, M., Doney, A.S.P., Eklund, N., Estrada, K., Eury, E., Folkerse, L., Fraser, R.M., Garcia, M.E., Geller, F., Giedraitis, V., Gigante, B., Go, A.S., Golay, A., Goodall, A.H., Gordon, S.D., Gorski, M., Grabe, H.-J., Grallert, H., Grammer, T.B., Gräfler, J., Grönberg, H., Groves, C.J., Gusto, G., Haessler, J., Hall, P., Haller, T., Hallmans, G., Hartman, C.A., Hassinen, M., Hayward, C., Heard-Costa, N.L., Helmer, Q., Hengstenberg, C., Holmen, O., Hottenga, J.-J., James, A.L., Jeff, J.M., Johansson, Å., Jolley, J., Juliusdottir, T., Kinnunen, L., Koenig, W., Koskenvuo, M., Kratzer, W., Laitinen, J., Lamina, C., Leander, K., Lee, N.R., Lichtner, P., Lind, L., Lindström, J., Lo, K.S., Lobbens, S., Lorbeer, R., Lu, Y., Mach, F., Magnusson, P.K.E., Mahajan, A., McArdle, W.L., McLachlan, S., Menni, C., Merger, S., Mihailov, E., Milani, L., Moayyeri, A., Monda, K.L., Morken, M.A., Mulas, A., Müller, G., Müller-Nurasyid, M., Musk, A.W., Nagaraja, R., Nöthen, M.M., Nolte, I.M., Pilz, S., Rayner, N.W., Renstrom, F., Rettig, R., Ried, J.S., Ripke, S., Robertson, N.R., Rose, L.M., Sanna, S., Scharnagl, H., Scholten, S., Schumacher, F.R., Scott, W.R., Seufferlein, T., Shi, J., Smith, A.V., Smolonska, J., Stanton, A.V., Steinthorsdottir, V., Stirrup, K., Stringham, H.M., Sundström, J., Swertz, M.A., Swift, A.J., Syvänen, A.-C., Tan, S.-T., Tayo, B.O., Thorand, B., Thorleifsson, G., Tyrer, J.P., Uh, H.-W., Vandendput, L., Verhulst, F.C., Vermeulen, S.H., Verweij, N., Vonk, J.M., Waite, L.L., Warren, H.R., Waterworth, D., Weedon, M.N., Wilkens, L.R., Willenborg, C., Wilsgaard, T., Wojczynski, M.K., Wong, A., Wright, A.F., Zhang, Q., LifeLines Cohort Study, Brennan, E.P., Choi, M., Dastani, Z., Drong, A.W., Eriksson, P., Franco-Cereceda, A., Gådin, J.R., Gharavi, A.G., Goddard, M.E., Handsaker, R.E., Huang, J., Karpe, F., Kathiresan, S., Keildson, S., Kiryluk, K., Kubo, M., Lee, J.-Y., Liang, L., Lifton, R.P., Ma, B., McCarroll, S.A., McKnight, A.J., Min, J.L., Moffatt, M.F., Montgomery, G.W., Murabito, J.M., Nicholson, G., Nyholt, D.R., Okada, Y., Perry, J.R.B., Dorajoo, R., Reimmaa, E., Salem, R.M., Sandholm, N., Scott, R.A., Stolk, L., Takahashi, A., Tanaka, Toshihiro, van 't Hooft, F.M., Vinkhuyzen, A.A.E., Westra, H.-J., Zheng, W., Zondervan, K.T., ADIPOGen Consortium, AGEN-BMI Working Group, CARDIOGRAMplusC4D Consortium, CKDGen Consortium, GLGC, ICBP, MAGIC Investigators, MuTHER Consortium, MiGen Consortium, PAGE Consortium, ReproGen Consortium, GENIE Consortium, International Endogene Consortium, Heath, A.C., Arveiler, D., Bakker, S.J.L., Beilby, J., Bergman, R.N., Blangero, J., Bovet, P., Campbell, H., Caulfield, M.J., Cesana, G., Chakravarti, A., Chasman, D.I.,

- Chines, P.S., Collins, F.S., Crawford, D.C., Cupples, L.A., Cusi, D., Danesh, J., de Faire, U., den Ruijter, H.M., Dominicak, A.F., Erbel, R., Erdmann, J., Eriksson, J.G., Farrall, M., Felix, S.B., Ferrannini, E., Ferrières, J., Ford, I., Forouhi, N.G., Forrester, T., Franco, O.H., Gansevoort, R.T., Gejman, P.V., Gieger, C., Gottesman, O., Gudnason, V., Gyllensten, U., Hall, A.S., Harris, T.B., Hattersley, A.T., Hicks, A.A., Hindorff, L.A., Hingorani, A.D., Hofman, A., Homuth, G., Hovingh, G.K., Humphries, S.E., Hunt, S.C., Hyppönen, E., Illig, T., Jacobs, K.B., Jarvelin, M.-R., Jöckel, K.-H., Johansen, B., Jousilahti, P., Jukema, J.W., Jula, A.M., Kaprio, J., Kastelein, J.J.P., Keinanen-Kiukaanniemi, S.M., Kiemeneij, L.A., Knekt, P., Kooperberg, C., Kovacs, P., Kraja, A.T., Kumari, M., Kuusisto, J., Lakka, T.A., Langenberg, C., Marchand, L., Lehtimäki, T., Lyssenko, V., Männistö, S., Marette, A., Matise, T.C., McKenzie, C.A., McKnight, B., Moll, F.L., Morris, A.D., Morris, A.P., Murray, J.C., Nelis, M., Ohlsson, C., Oldehinkel, A.J., Ong, K.K., Madden, P.A.F., Pasterkamp, G., Peden, J.F., Peters, A., Postma, D.S., Pramstaller, P.P., Price, J.F., Qi, L., Raitakari, O.T., Rankinen, T., Rao, D.C., Rice, T.K., Ridker, P.M., Rioux, J.D., Ritchie, M.D., Rudan, I., Salomaa, V., Samani, N.J., Saramies, J., Sarzynski, M.A., Schunkert, H., Schwarz, P.E.H., Sever, P., Shuldiner, A.R., Sinisalo, J., Stolk, R.P., Strauch, K., Tönjes, A., Trégouët, D.-A., Tremblay, A., Tremoli, E., Virtamo, J., Vohl, M.-C., Völker, U., Waeber, G., Willemsen, G., Witteman, J.C., Zillikens, M.C., Adair, L.S., Amouyel, P., Asselbergs, F.W., Assimes, T.L., Bochud, M., Boehm, B.O., Boerwinkle, E., Bornstein, S.R., Bottinger, E.P., Bouchard, C., Cauchi, S., Chambers, J.C., Chanock, S.J., Cooper, R.S., de Bakker, P.I.W., Dedoussis, G., Ferrucci, L., Franks, P.W., Froguel, P., Groop, L.C., Haiman, C.A., Hamsten, A., Hui, J., Hunter, D.J., Hveem, K., Kaplan, R.C., Kivimaki, M., Kuh, D., Laakso, M., Liu, Y., Martin, N.G., März, W., Melbye, M., Metspalu, A., Moebus, S., Munroe, P.B., Njølstad, I., Oostra, B.A., Palmer, C.N.A., Pedersen, N.L., Perola, M., Pérusse, L., Peters, U., Power, C., Quertermous, T., Rauramaa, R., Rivadeneira, F., Saaristo, T.E., Saleheen, D., Sattar, N., Schadt, E.E., Schlessinger, D., Slagboom, P.E., Snieder, H., Spector, T.D., Thorsteinsdóttir, U., Stumvoll, M., Tuomilehto, J., Uitterlinden, A.G., Usutupa, M., van der Harst, P., Walker, M., Wallschafski, H., Wareham, N.J., Watkins, H., Weir, D.R., Wichmann, H.-E., Wilson, J.F., Zanen, P., Borecki, I.B., Deloukas, P., Fox, C.S., Heid, I.M., O'Connell, J.R., Strachan, D.P., Stefansson, K., van Duijn, C.M., Abecasis, G.R., Franke, L., Frayling, T.M., McCarthy, M.I., Visscher, P.M., Scherag, A., Willer, C.J., Boehnke, M., Mohlke, K.L., Lindgren, C.M., Beckmann, J.S., Barroso, I., North, K.E., Ingelsson, E., Hirschhorn, J.N., Loos, R.J.F., Speliotes, E.K., 2015. Genetic studies of body mass index yield new insights for obesity biology. *Nature* 518, 197–206.
- Mardakheh, F.K., Auciello, G., Dafforn, T.R., Rappoport, J.Z., Heath, J.K., 2010. Nbr1 is a novel inhibitor of ligand-mediated receptor tyrosine kinase degradation. *Mol. Cell Biol.* 30, 5672–5685.
- Mayya, V., Lundgren, D.H., Hwang, S.-I., Rezaul, K., Wu, L., Eng, J.K., Rodionov, V., Han, D.K., 2009. Quantitative phosphoproteomic analysis of T cell receptor signaling reveals system-wide modulation of protein-protein interactions. *Sci. Signal.* 2, ra46.
- McMahon, K.W., Hirsch, B.A., MacDonald, C.C., 2006. Differences in polyadenylation site choice between somatic and male germ cells. *BMC Mol. Biol.* 7, 1–11.
- McNab, F., Mayer-Barber, K., Sher, A., Wack, A., O'Garra, A., 2015. Type I interferons in infectious disease. *Nat. Rev. Immunol.* 15, 87–103.
- Mossadeq-Keller, N., Sieweke, M.H., 2018. Testicular macrophages: guardians of fertility. *Cell. Immunol.* 330, 120–125.
- Motwani, M., Pesirisidis, S., Fitzgerald, K.A., 2019. DNA sensing by the cGAS-STING pathway in health and disease. *Nat. Rev. Genet.* 20, 657–674.
- Mueller, T.D., Feigon, J., 2002. Solution structures of UBA domains reveal a conserved hydrophobic surface for protein-protein interactions. *J. Mol. Biol.* 319, 1243–1255.
- Muraro, M.J., Dharmadhikari, G., Grün, D., Groen, N., Dielen, T., Jansen, E., van Gurp, L., Engelse, M.A., Carlotti, F., de Koning, E.J.P., van Oudenaarden, A., 2016. A single-cell transcriptome atlas of the human pancreas. *Cell Syst.* 3, 385–394 e3.
- Nance, T., Smith, K.S., Anaya, V., Richardson, R., Ho, L., Pala, M., Mostafavi, S., Battle, A., Feghali-Bostwick, C., Rosen, G., Montgomery, S.B., 2014. Transcriptome analysis reveals differential splicing events in IPF lung tissue. *PLoS One* 9, e92111.
- Nguyen, T.P., Bazzar, D.A., Mudd, J.C., Lederman, M.M., Harding, C.V., Hardy, G.A., Sieg, S.F., 2015. Interferon- α inhibits CD4 T cell responses to interleukin-7 and interleukin-2 and selectively interferes with Akt signaling. *J. Leukoc. Biol.* 97, 1139–1146.
- Nguyen, N.T.H., Now, H., Kim, W.J., Kim, N., Yoo, J.Y., 2016. Ubiquitin-like modifier FAT10 attenuates RIG-I mediated antiviral signaling by segregating activated RIG-I from its signaling platform. *Sci. Rep.* 6, 1–12.
- Olsen, J.V., Vermeulen, M., Santamaría, A., Kumar, C., Miller, M.L., Jensen, L.J., Gnad, F., Cox, J., Jensen, T.S., Nigg, E.A., Brunak, S., Mann, M., 2010. Quantitative phosphoproteomics reveals widespread full phosphorylation site occupancy during mitosis. *Sci. Signal.* 3, ra3.
- Osokine, I., Snell, L.M., Cunningham, C.R., Yamada, D.H., Wilson, E.B., Elsaesser, H.J., De La Torre, J.C., Brooks, D., 2014. Type i interferon suppresses de novo virus-specific CD4 Th1 immunity during an established persistent viral infection. *Proc. Natl. Acad. Sci. U. S. A.* 111, 7409–7414.
- Pai, A.A., Baharian, G., Paggi Sabourin, A., Brinkworth, J.F., Nédélec, Y., Foley, J.W., Grenier, J.C., Siddle, K.J., Dumaine, A., Yotova, V., Johnson, Z.P., Lanford, R.E., Burge, C.B., Barreiro, L.B., 2016. Widespread shortening of 3' untranslated regions and increased exon inclusion are evolutionarily conserved features of innate immune responses to infection. *PLoS Genet.* 12, 1–24.
- Park, S.H., Kang, Kyuho, Giannopoulou, E., Qiao, Y., Kang, Keunsoo, Kim, G., Park-Min, K.-H., Ivashkiv, L.B., 2017. Type I interferons and the cytokine TNF cooperatively reprogram the macrophage epigenome to promote inflammatory activation. *Nat. Immunol.* 18, 1104–1116.
- Pettersen, E.F., Goddard, T.D., Huang, C.C., Couch, G.S., Greenblatt, D.M., Meng, E.C., Ferrin, T.E., 2004. UCSF Chimera—a visualization system for exploratory research and analysis. *J. Comput. Chem.* 25, 1605–1612.
- Quinn, E.M., Coleman, C., Molloy, B., Castro, P.D., Cormican, P., Trimble, V., Mahmud, N., McManus, R., 2015. Transcriptome analysis of CD4+ T cells in coeliac disease reveals imprint of BACH2 and IFNI regulation. *PLoS One* 10, 1–25.
- Rao, T., Gao, R., Takada, S., Al Abo, M., Chen, X., Walters, K.J., Pommier, Y., Aihara, H., 2016. Novel TDP-2 ubiquitin interactions and their importance for the repair of topoisomerase II-mediated DNA damage. *Nucleic Acids Res.* 44, gkw719.
- Ribbolt, K.T.G., Prokhorova, T.A., Akimov, V., Henningsen, J., Johansen, P.T., Kratchmarova, I., Kassem, M., Mann, M., Olsen, J.V., Blagoev, B., 2011. System-wide temporal characterization of the proteome and phosphoproteome of human embryonic stem cell differentiation. *Sci. Signal.* 4, rs3.
- Riveros-McKay, F., Mistry, V., Bounds, R., Hendricks, A., Keogh, J.M., Thomas, H., Henning, E., Corbin, L.J., O'Rahilly, S., Zeggini, E., Wheeler, E., Barroso, I., Farooqi, I.S., 2019. Genetic architecture of human thinness compared to severe obesity. *PLoS Genet.* 15, e1007603.
- Rodero, M.P., Crow, Y.J., 2016. Type I interferon-mediated monogenic autoinflammation: the type I interferonopathies, a conceptual overview. *J. Exp. Med.* 213, 2527–2538.
- Ruterding, J., Ilmer, M., Recio, A., Coleman, M., Vykovakal, J., Alt, E., Orleans, N., 2016. Partial exhaustion of CD8 T cells and clinical response to teplizumab in new-onset type 1 diabetes. *Sci. Immunol.* 5, 1–8.
- Saeki, Y., 2017. Ubiquitin recognition by the proteasome. *J. Biochem.* 161, mvw091.
- SEQC/MAQC-III Consortium, 2014. A comprehensive assessment of RNA-seq accuracy, reproducibility and information content by the Sequencing Quality Control Consortium. *Nat. Biotechnol.* 32, 903–914.
- Shen, J., Xiao, Z., Zhao, Q., Li, M., Wu, X., Zhang, L., Hu, W., Cho, C.H., 2018. Anti-cancer therapy with TNF α and IFN γ : a comprehensive review. *Cell Prolif.* 51, e12441.
- Singh, R.N., Singh, N.N., 2019. A novel role of U1 snRNP: splice site selection from a distance. *Biochim. Biophys. Acta - Gene Regul. Mech.* 1862, 634–642.
- Skupien-Rabian, B., Jankowska, U., Swiderska, B., Lukasiewicz, S., Ryszawy, D., Dziedzicka-Wasylewska, M., Kedracka-Krok, S., 2016. Proteomic and bioinformatic analysis of a nuclear intrinsically disordered proteome. *J. Proteomics* 130, 76–84.
- Smart, O.S., Womack, T.O., Flensburg, C., Keller, P., Paciorek, W., Sharff, A., Vonrhein, C., Bricogne, G., 2012. Exploiting structure similarity in refinement: automated NCS and target-structure restraints in BUSTER. *Acta Crystallogr. D. Biol. Crystallogr.* 68, 368–380.
- Snell, L.M., McGaha, T.L., Brooks, D.G., 2017. Type I interferon in chronic virus infection and cancer. *Trends Immunol.* 38, 542–557.
- Sood, A.K., Kim, H., Gerards, J., 2012. PDEF in prostate cancer. *Prostate* 72, 592–596.
- Sovio, U., Bennett, A.J., Millwood, L.Y., Molitor, John, O'Reilly, P.F., Timson, J.N., Kaakinen, M., Laitinen, J., Haukka, J., Pillas, D., Tzoulaki, I., Molitor, Jassy, Hoggart, C., Coin, L.J.M., Whittaker, J., Pouta, A., Hartikainen, A.L., Freimer, N.B., Widen, E., Peltonen, L., Elliott, P., McCormathy, M., Jarvelin, M.R., 2009. Genetic determinants of height growth assessed longitudinally from infancy to adulthood in the northern Finland birth cohort 1966. *PLoS Genet.* 5, 1–8.
- Srikiatkachorn, A., Mathew, A., Rothman, A.L., 2017. Immune-mediated cytokine storm and its role in severe dengue. *Semin. Immunopathol.* 39, 563–574.
- Stetson, D.B., Medzhitov, R., 2006. Type I interferons in host defense. *Immunity* 25, 373–381.
- Swann, J.B., Hayakawa, Y., Zerafa, N., Sheehan, K.C.F., Scott, B., Schreiber, R.D., Hertzog, P., Smyth, M.J., 2007. Type I IFN contributes to NK cell homeostasis, activation, and antitumor function. *J. Immunol.* 178, 7540–7549.
- Swatek, K.N., Komander, D., 2016. Ubiquitin modifications. *Cell Res.* 26, 399–422.
- Swiecki, M., Colonna, M., 2015. The multifaceted biology of plasmacytoid dendritic cells. *Nat. Rev. Immunol.* 15, 471–485.
- Tanaka, T., Narazaki, M., Kishimoto, T., 2014. IL-6 in inflammation, immunity, and disease. *Cold Spring Harb. Perspect. Biol.* 6, a016295.
- Theurich, S., Tsaoisidou, E., Hanssen, R., Lempradl, A.M., Mauer, J., Timper, K., Schilbach, K., Folz-Donahue, K., Heilinger, C., Sexl, V., Pospisil, J.A., Wunderlich, F.T., Brüning, J.C., 2017. IL-6/Stat3-Dependent induction of a distinct, obesity-associated NK cell subpopulation deteriorates energy and glucose homeostasis. *Cell Metabol.* 26, 171–184 e6.
- Tickle, L.J., Flensburg, C., Keller, P., Paciorek, W., Sharff, A., Vonrhein, C., Bricogne, G., 2018. STARANISO.
- Tompa, P., Schad, E., Tantos, A., Kalmar, L., 2015. Intrinsically disordered proteins: emerging interaction specialists. *Curr. Opin. Struct. Biol.* 35, 49–59.
- Trimarchi, T., Bilal, E., Ntziaachristos, P., Fabbri, G., Dalla-Favera, R., Tsirigos, A., Aifantis, I., 2014. Genome-wide mapping and characterization of Notch-regulated long noncoding RNAs in acute leukemia. *Cell* 158, 593–606.
- Vecchio, F., Buono, N. Lo, Stabilini, A., Nigi, L., Dufort, M.J., Geyer, S., Rancoita, P.M., Cugnata, F., Mandelli, A., Valle, A., Leete, P., Mancarella, F., Linsley, P.S., Krogvold, L., Herold, K.C., Larsson, H.E., Richardson, S.J., Morgan, N.G., Dahl-Jorgenson, K., 2018. Abnormal neutrophil signature in the blood and pancreas of presymptomatic and symptomatic type 1 diabetes Federica Vecchio, the Type 1 Diabetes TrialNet Study Group , Manuela Battaglia Find the latest version : abnormal neutrophil signature in the bl. *JCI Insight* 3, 1–17.
- van der Veen, A.G., Ploegh, H.L., 2012. Ubiquitin-like proteins. *Annu. Rev. Biochem.* 81, 323–357.
- Venken, K., Jacques, P., Mortier, C., Labadia, M.E., Decruy, T., Coudenys, J., Hoyt, K., Wayne, A.L., Hughes, R., Turner, M., Van Gassen, S., Martens, L., Smith, D., Harcken, C., Wahle, J., Wang, C.T., Verheugen, E., Schryvers, N., Varkas, G., Cyders, H., Wittoek, N., Piette, Y., Gyselbrecht, L., Van Calenbergh, S., Van den Bosch, F., Saeyns, Y., Nabozny, G., Elewaut, D., 2019. ROR γ t inhibition selectively

- targets IL-17 producing iNKT and $\gamma\delta$ -T cells enriched in Spondyloarthritis patients. *Nat. Commun.* 10.
- Vonrhein, C., Flensburg, C., Keller, P., Sharff, A., Smart, O., Paciorek, W., Womack, T., Bricogne, G., 2011. Data processing and analysis with the autoPROC toolbox. *Acta Crystallogr. D. Biol. Crystallogr.* 67, 293–302.
- Wang, Q., Goh, A.M., Howley, P.M., Walters, K.J., 2003. Ubiquitin recognition by the DNA repair protein hHR23a. *Biochemistry* 42, 13529–13535.
- Wang, H., Sartini, B.L., Millette, C.F., Kilpatrick, D.L., 2006. A developmental switch in transcription factor isoforms during spermatogenesis controlled by alternative messenger RNA 3'-end Formation1. *Biol. Reprod.* 75, 318–323.
- Wang, F., Marshall, C.B., Ikura, M., 2013. Transcriptional/epigenetic regulator CBP/p300 in tumorigenesis: structural and functional versatility in target recognition. *Cell. Mol. Life Sci.* 70, 3989–4008.
- Wenric, S., ElGuendi, S., Caberg, J.-H., Bezzaou, W., Fasquelle, C., Charlotteaux, B., Karim, L., Hennuy, B., Frères, P., Collignon, J., Boukerroucha, M., Schroeder, H., Olivier, F., Jossa, V., Jerusalem, G., Josse, C., Bours, V., 2017. Transcriptome-wide analysis of natural antisense transcripts shows their potential role in breast cancer. *Sci. Rep.* 7, 17452.
- Williams, C.J., Headd, J.J., Moriarty, N.W., Prisant, M.G., Videau, L.L., Deis, L.N., Verma, V., Keedy, D.A., Hintze, B.J., Chen, V.B., Jain, S., Lewis, S.M., Arendall, W.B., Snoeyink, J., Adams, P.D., Lovell, S.C., Richardson, J.S., Richardson, D.C., 2018. MolProbity: more and better reference data for improved all-atom structure validation. *Protein Sci.* 27, 293–315.
- Winn, M.D., Ballard, C.C., Cowtan, K.D., Dodson, E.J., Emsley, P., Evans, P.R., Keegan, R.M., Krissinel, E.B., Leslie, A.G.W., McCoy, A., McNicholas, S.J., Murshudov, G.N., Pannu, N.S., Potterton, E.A., Powell, H.R., Read, R.J., Vagin, A., Wilson, K.S., 2011. Overview of the CCP4 suite and current developments. *Acta Crystallogr. D. Biol. Crystallogr.* 67, 235–242.
- Wright, P.E., Dyson, H.J., 2015. Intrinsically disordered proteins in cellular signalling and regulation. *Nat. Rev. Mol. Cell Biol.* 16, 18–29.
- Xu, D., Zhang, Y., 2012. Ab initio protein structure assembly using continuous structure fragments and optimized knowledge-based force field. *Proteins* 80, 1715–1735.
- Xu, D., Zhang, Y., 2013. Toward optimal fragment generations for ab initio protein structure assembly. *Proteins* 81, 229–239.
- Xu, J., Lee, J.W., Park, S.K., Lee, S.B., Yoon, Y.H., Yeon, S.H., Rha, K.S., Choi, J.A., Song, C.H., Kim, Y.M., 2018. Toll-like receptor 9 ligands increase type I interferon induced B-cell activating factor expression in chronic rhinosinusitis with nasal polypsis. *Clin. Immunol.* 197, 19–26.
- Younan, P., Iampietro, M., Nishida, A., Ramanathan, P., Santos, R.I., Dutta, M., Lubaki, N.M., Koup, R.A., Katze, M.G., Bukreyev, A., 2017. Ebola virus binding to tim-1 on T lymphocytes induces a cytokine storm. *MBio* 8.
- Yu, B., Russanova, V.R., Gravina, S., Hartley, S., Mullikin, J.C., Ignezewski, A., Graham, J., Segars, J.H., DeCherney, A.H., Howard, B.H., 2015. DNA methylome and transcriptome sequencing in human ovarian granulosa cells links age-related changes in gene expression to gene body methylation and 3'-end GC density. *Oncotarget* 6, 3627–3643.
- Zhang, X., Miao, Y., Yu, X., Zhang, Y., Jiang, G., Liu, Y., Yu, J., Han, Q., Zhao, H., Wang, E., 2015. C6orf106 enhances NSCLC cell invasion by upregulating vimentin, and downregulating E-cadherin and P120ctn. *Tumor Biol.* 36, 5979–5985.
- Zhao, J., Li, M., Bradfield, J.P., Zhang, H., Mentch, F.D., Wang, K., Sleiman, P.M., Kim, C.E., Glessner, J.T., Hou, C., Keating, B.J., Thomas, K.A., Garris, M.L., Deliard, S., Frackleton, E.C., Otieno, F.G., Chiavacci, R.M., Berkowitz, R.I., Hakonarson, H., Grant, S.F.A., 2010. The role of height-associated loci identified in genome wide association studies in the determination of pediatric stature. *BMC Med. Genet.* 11.
- Zhou, H., Di Palma, S., Preisinger, C., Peng, M., Polat, A.N., Heck, A.J.R., Mohammed, S., 2013. Toward a comprehensive characterization of a human cancer cell phosphoproteome. *J. Proteome Res.* 12, 260–271.
- Zitvogel, L., Galluzzi, L., Kepp, O., Smyth, M.J., Kroemer, G., 2015. Type I interferons in antitumor immunity. *Nat. Rev. Immunol.* 15, 405–414.